

# How Resonances can synchronise with Thresholds

D. V. Bugg<sup>1</sup>

Queen Mary, University of London, London E1 4NS, UK

## Abstract

The mechanism by which a threshold may capture a resonance is examined. It involves a threshold cusp interfering constructively with either or both (i) a resonance produced via confinement, (ii) attractive  $t$ - and  $u$ -channel exchanges. The  $f_0(980)$ ,  $X(3872)$  and  $Z(4430)$  are studied in detail. The  $f_0(980)$  provides a valuable model of the locking mechanism. The  $X(3872)$  is too narrow to be fitted by a cusp, and requires either a resonance or virtual state. The  $Z(4430)$  can be fitted as a resonance but also can be fitted successfully by a cusp with no nearby resonant pole.

PACS numbers: 12.39.Mk, 13.25.Gv, 13.25.Hw, 14.40.Lb, 14.40.Nd

## 1 Introduction

It is well known that several meson resonances appear at or close to thresholds. Examples are  $f_0(980)$  and  $a_0(980)$  at the  $KK$  threshold,  $f_2(1565)$  at the  $\omega\omega$  threshold and  $K_0(1430)$  close to the  $K\eta'$  threshold. In all these cases, decays to mesons are via S-waves. Further possible examples are  $X(3872)$  at the  $\bar{D}(1865)D^*(2007)$  threshold,  $Z(4430)$  close to the  $D^*(2007)\bar{D}_1(2420)$  threshold and  $Y(4260)$  close to the  $D(1865)\bar{D}_1(2420)$  threshold. [The  $\bar{D}D$  charge conjugate combination is tacitly included throughout this paper]. Amongst baryons,  $P_{11}(1710)$  and  $P_{13}(1720)$  appear close to the  $N\omega$  threshold (1720 MeV), and  $\Lambda_C(2940)$  appears close to the  $D^*(2007)N$  threshold.

All these cases have been discussed as ‘molecules’, bound a few MeV below the thresholds. There is much argument whether they should be viewed as bound states of mesons or as quark configurations, e.g.  $c\bar{c}n\bar{n}$  in the case of  $X(3872)$ .

The first objective of this paper is to draw attention to a known but frequently overlooked mechanism which attracts resonances to thresholds. The  $f_0(980)$  is studied in depth as one specimen. The second objective is to point out the role of zero-point energy. This provides some distinction between mesonic molecules (uncoloured) and quark configurations, which are coloured and therefore confined. Thirdly, an improved but convenient form of the Flatté formula [1] is proposed for the case of sharp thresholds like  $KK$  and other cases cited above.

Consider as an example  $f_0(980)$  and its decay to  $KK$ . The conventional Flatté denominator for this resonances is

$$D(s) = M^2 - s - i \sum_i \Pi_i, \quad (1)$$

where  $M$  is resonance mass,  $\text{Im } \Pi_i = g_i^2 \rho_i$ ,  $g_i^2$  are coupling constants to decay channels and  $\rho_i$  are phase space factors. However, further dispersive terms  $\text{Re } \Pi_i(s)$  are required in  $D(s)$ :

$$- \text{Re } \Pi_i(s) = -\frac{1}{\pi} \text{P} \int_{4m_i^2}^{\infty} ds' \frac{g_i^2(s') \rho_i(s')}{s' - s}, \quad (2)$$

---

<sup>1</sup>email: d.bugg@rl.ac.uk

where  $m_i$  are  $\pi$  and  $K$  masses and  $P$  denotes the principal value integral. In fact, the terms  $ig_i^2\rho_i$  of Eq. (1) arise from the pole at  $s' = s$  in Eq. (2).

Fig. 1 shows  $\Pi_{KK}(s)$  and  $g_{KK}^2\rho_{KK}(s)$  near the  $KK$  threshold, using a form factor  $e^{-3k^2}$ , where  $k$  is centre of mass  $KK$  momentum in GeV/c. There is a cusp in  $\Pi(s)_{KK}$  at the threshold. The fact that it is positive definite at threshold signifies additional attraction appearing there. A minor technicality is that  $\Pi(s)$  goes negative after the peak in  $\rho(s)$ , since the dispersion integral is close to the gradient of  $\rho(s)$ . Eventually it returns slowly to zero for large  $s$ .

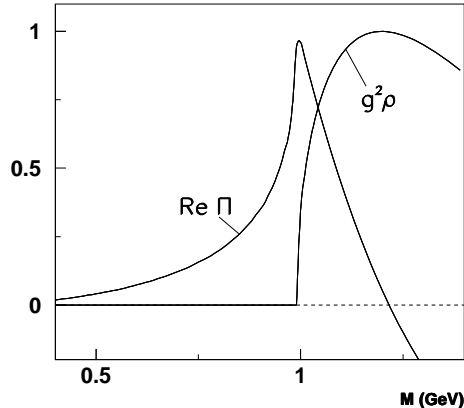


Figure 1:  $\text{Re}\Pi_{KK}(s)$  and  $g_{KK}^2\rho_{KK}(s)$  for  $f_0(980)$ , normalised to 1 at the peak of  $g_{KK}^2\rho_{KK}$ .

If the cusp is superimposed on attraction from another source, for example meson exchanges, a resonance can be generated by the peak in  $\text{Re}\Pi$ ; if the attraction is not quite sufficient to produce a resonance, there is a virtual state instead. The  $\sigma$ ,  $\kappa$ ,  $a_0(980)$  and  $f_0(980)$  make good candidates for such molecules. Otherwise, all known cases except  $Z(4430)$  can conservatively be accommodated as regular quark resonances whose masses have been perturbed to synchronise with thresholds.

Near threshold, the wave function of the resonance has a long tail, like the deuteron. The long-range tail is purely mesonic; any contribution to the wave function from coloured quarks is confined in the resonance at short range or in the decay mesons. In the confined part of the wave function, quarks have kinetic energy  $k^2/2m = -(\hbar^2/2m)\nabla^2\Psi$ ; here  $k$  and  $m$  are quark momentum and effective mass and  $\Psi$  is the wave function. If a bound state is to be created, extra potential energy is needed to compensate the kinetic energy of the confined particles. This again pulls the resonance towards the threshold.

Jaffe proposed that the  $f_0(980)$  and  $a_0(980)$  are members of a 4-quark nonet with composition  $s\bar{s}(u\bar{u} \pm d\bar{d})$  [2]. This may be correct, but a long-range tail of  $KK$  is unavoidable.

Section 2 reviews the formalism. This leans heavily on a perceptive paper of Törnqvist [3], written in 1995, before many of the examples cited above were known or accurately measured. For the case of  $Z(4430)$ , some changes need to be introduced into his formalism.

Section 3 examines the  $f_0(980)$  in detail. Perturbations around its fitted parameters illustrate the general way in which a threshold captures a resonance. Section 4 examines  $X(3872)$ , which peaks within 0.6 MeV of the  $\bar{D}D^*$  threshold. It could be a mesonic molecule, as Törnqvist [4], Close and Page [5] and Swanson [6] have argued. Its very close relation to the threshold points strongly to the cusp mechanism playing a decisive role. A likely possibility is that the  $\bar{c}c$   $^3P_1$  radial excitation has been captured by the  $\bar{D}D^*$  threshold. If that state were to appear

elsewhere, the alternative explanation is a mesonic molecule or virtual state. Present data simply require a second-sheet pole.

The  $Z^+(4430)$  reported by Belle [7] appears as a peak in the  $\Psi'\pi^\pm$  mass spectrum in  $B \rightarrow \Psi'\pi^\pm K$ . The remarkable feature of this peak is that it has isospin 1, unlike regular  $c\bar{c}$  states, so it is exotic. Belle fit it as a resonance with mass  $M = 4433 \pm 4 \pm 1$  MeV and width  $\Gamma = 44_{-13}^{+17+30}_{-11}$  MeV. Rosner [8] and also Meng and Chao [9] point out that its mass is close to that of  $D^*(2010) + \bar{D}_1(2420)$ . Maiani et al. [10] interpret the peak as a diquark-antidiquark state. For an S-wave  $D^*\bar{D}_1$  combination, its spin-parity  $J^P$  is  $0^-, 1^-$  or  $2^-$ . It is discussed in detail in Section 5. It is easily fitted as a resonance. However, it can also be fitted as a cusp due to strong de-excitation of  $D^*(2010)\bar{D}_1(2420)$  to lower configurations of  $D\bar{D}$  and  $D^*\bar{D}$ .

Section 6 makes remarks about a number of the other states associated with thresholds, so as to fill in the broader picture. Section 7 summarises conclusions.

## 2 How to parametrise a cusp or threshold resonance

Törnqvist's formalism [3] will be followed here with some modifications. He considers the possibility of overlapping resonances such as  $f_0(980)$  and  $f_0(1370)$ ; that is a detail not required here, simplifying the notation. His formula for the amplitude connecting channels  $i$  and  $j$  (e.g.  $\pi\pi$  and  $KK$ ) is then

$$A_{ij}(s) = T_{ij}(s)\sqrt{\rho_i\rho_j} = G_i^\dagger(s)PG_j(s), \quad (3)$$

where  $P$  is the propagator;  $T$  is the usual  $T$ -matrix with phase space factored out. The  $G_i$  are related to coupling constants  $g_i$  via

$$G_i^2(s) = g_i^2\rho_i(s)F_i^2(s)\theta(s - s_{th,i}), \quad (4)$$

with  $s_{th,i}$  the threshold for channel  $i$ ;  $F_i(s)$  is a form factor, taken here as  $\exp(-k^2R^2/6)$  with  $R = 0.6$  fm. Then  $F^2 \simeq \exp(-3k^2)$  with  $k$  in GeV/c. For narrow resonances, the precise  $s$ -dependence of  $F^2$  is not decisive but begins to matter for broader structures like  $Z(4430)$ .

For a resonance,

$$P^{-1}(s) = M^2 - s - \Pi(s). \quad (5)$$

The definition of  $\Pi$  has the opposite sign to that used by Törnqvist, to avoid a multiplicity of minus signs in formulae which follow. The unitarity relation  $\text{Im } A = AA^\dagger$  gives

$$\text{Im } \Pi(s) = \sum_i g_i^2\rho_i(s)F_i^2(s)\theta(s - s_{th,i}). \quad (6)$$

Using analyticity,

$$\text{Re } \Pi(s) = \frac{1}{\pi}P \int_{s_{th,i}}^\infty ds' \frac{\text{Im } \Pi(s')}{s' - s}. \quad (7)$$

The term inside the summation of Eq. (6) is positive definite, leading always to attraction at and below threshold, though the dispersion integral can change sign above threshold.

## 2.1 Useful resonance formulae

If  $F^2(s) = 1$ , the integral in (7) diverges. However, with two subtractions, it can be evaluated analytically with the result [12]

$$\frac{\text{Re } \Pi(s)_i}{g_i^2} = j_i = \frac{\rho_i}{\pi} \ln \frac{1 - \rho_i}{1 + \rho_i}, \quad s \geq s_{th,i} \quad (8)$$

$$= -\sqrt{\frac{4m_i^2 - s}{s}} - \frac{2v_i}{\pi} \tan^{-1} v_i, \quad s < s_{th,i} \quad (9)$$

where

$$\rho_i = 2k_i/\sqrt{s}, \quad s \geq s_{th,i} \quad (10)$$

$$v_i = 2|k_i|/\sqrt{s}, \quad s < s_{th,i} \quad (11)$$

and  $k_i$  are momenta of decay particles in the rest frame of the resonance. The first term of Eq. (9) is the usual Flatté extrapolation below threshold. The contributions to  $j_i$  near threshold from remaining terms are

$$\pi j_i = -2\rho_i^2 - (2/3)\rho_i^4 + \dots, \quad s \geq s_{th,i} \quad (12)$$

$$= -2v_i^2 + (2/3)v_i^4 + \dots, \quad s < s_{th,i}. \quad (13)$$

The first term in each is symmetrical about threshold, but the next term leads to an asymmetry away from the threshold. It is also important to realise that the two subtractions used in arriving at this result allow  $\Pi_i$  to contain an additional linear dependence on  $s$ . A constant term is certainly required to make the integral of (7) positive at threshold.

In illustrations given later, the principal value integral will be evaluated numerically. However, the algebraic forms (8) and (9) improve on the usual Flatté form for a resonance near threshold, but are equally convenient to use. A constant term can be absorbed into  $M^2$  of the Breit-Wigner amplitude giving

$$D(s) = M^2 - s - \sum_i g_i^2 (j_i + i\rho_i). \quad (14)$$

For small  $v_2^2$  below the opening threshold, the second term of Eq. (9) contributes

$$\frac{2}{\pi} g_2^2 v_2^2 = \frac{2g_2^2}{\pi} \left( \frac{4m_K^2 - s}{s} \right). \quad (15)$$

Note the explicit appearance of the factor  $(4m_K^2 - s)$  in equation (15) and also in the first term of Eq. (9). The cusp mechanism is contributing to the resonance through a term like  $(M^2 - s)$  but peaking at the threshold. Also note that, when fitting data, there is a strong correlation between the term  $M^2 - s$  and  $-g_2^2 j_2$ . If there are no data on the  $KK$  channel to determine  $g_2^2$  directly, data below the  $KK$  threshold give almost no determination of  $g_2^2$  in view of the poorly known form factor  $F_2^2$ .

The fit to BES data on  $J/\Psi \rightarrow \phi\pi^+\pi^-$  and  $\phi K^+K^-$  [11] changes very little when the Flatté formula is replaced by Eq. (9). The  $\phi KK$  data determine  $g_2^2$  well, and a modest change in  $M^2$  compensates for the change in the formula.

If there is a linear subtraction term in addition to the constant term,

$$D(s) \rightarrow M^2 - (1 + \beta)s - \sum_i g_i^2(j_i + i\rho_i) \quad (16)$$

$$= (1 + \beta) \left[ \frac{M^2}{1 + \beta} - s - \frac{1}{1 + \beta} \sum_i g_i^2(j_i + i\rho_i) \right]. \quad (17)$$

This leads to a renormalisation of the mass and width, as observed for  $f_0(1370)$  in a recent re-analysis including dispersive terms arising from the opening of the  $4\pi$  channel [13]. For practical purposes, the factor  $1/(1 + \beta)$  renormalises mass and width terms in (17).

## 2.2 No resonance and approach to resonance

If there is no resonance, it is convenient to replace  $M^2 - s$  of (14) by a constant  $M^2$ , hence keeping dimensions unchanged. In Section 5, it will be shown that the K-matrix approach leads to further terms neglected by Törnqvist, but they can safely be ignored in the cases of  $f_0(980)$  and  $X(3872)$ . Standard effective range theory replaces  $M^2$  by  $M^2 - \gamma k^2$ . As  $\gamma$  increases, a virtual state approaches the threshold and smoothly becomes a bound state - or resonance if there are open channels.

The cusp mechanism gives maximum attraction at the threshold. A resonance close to threshold necessarily has a long-range tail, mesonic in character. Consider as an example mixing between  $c\bar{c}$  and a  $(c\bar{n})(\bar{c}n)$  configuration, appropriate to the discussion of  $X(3872)$ . The mixing is given by the familiar eigenvalue equation

$$H\Psi = \begin{pmatrix} H_{11} & V \\ V & H_{22} \end{pmatrix} \Psi, \quad (18)$$

where  $H_{11}$  and  $H_{22}$  describe isolated  $c\bar{c}$  and  $(c\bar{n})(\bar{c}n)$  configurations and  $V$  describes mixing. This mixing pushes the  $c\bar{c}$  state down in mass. This is the well known Variational Principle which minimises the eigenvalue when states mix. It is closely analogous to formation of a covalent bond in chemistry. The  $c\bar{n}$  configuration is different in detail from an atom made of a proton and electron, but the principle is the same. The detailed dynamics of the decay of a confined state through the confining barrier is a key missing detail at present; so is the possible role of di-quark interactions in the ‘molecule’.

The meson-meson component has  $t$  or  $u$  channel poles, but slow variation with  $s$ . The linear combination with  $c\bar{c}$  has minimum zero-point energy when the resonance is centred on the threshold *and* is narrow. Both the cusp attraction at threshold and the effect of zero-point energy provide feedback tending to lock the resonance to the threshold. In the next section, the  $f_0(980)$  will be used as a model to examine this locking mechanism numerically.

The dispersive effect at the threshold may be an unfamiliar effect. Vacuum polarisation arises in this way. An example from classical physics is a tsunami - a travelling cusp. As a tsunami approaches a beach, attraction into the wave-front drains water from the beach well in advance of the wave and gives advance warning of the approaching wave.

### 3 The $f_0(980)$

Can we be sure that the  $f_0(980)$  is really a resonance and not a virtual state or cusp? Cern-Munich data on  $\pi\pi$  elastic scattering [14] were first fitted to a simple Breit-Wigner resonance of constant width and yielded a good fit with a phase increase of  $\sim 180^\circ$  over the  $KK$  threshold. Crystal Barrel data on  $\bar{p}p \rightarrow 3\pi^0$  are a further delicate source of information [15]. The  $f_0(980)$  appears as a visible dip in the  $\pi\pi$  mass projection. These data provide accurate phase information on  $f_0(980)$  via interferences between the three  $\pi^0\pi^0$  combinations all over the Dalitz plot.

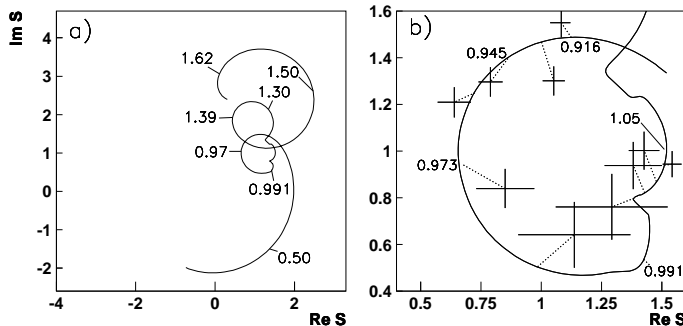


Figure 2: (a) The Argand diagram for the  $\pi\pi$  S-wave from [13], (b) enlarged comparison with the  $f_0(980)$  mass region; crosses indicate errors for free fits to real and imaginary parts of the amplitude in 10 equal bins of  $s$  from 0.84 to 1.08  $\text{GeV}^2$ ; dotted lines indicate the movement of free fits from that with a Flatté formula; numbers indicate masses in  $\text{GeV}$ .

Fig. 2(a) shows the Argand plot of the  $\pi\pi$  S-wave amplitude from a recent re-analysis of the data [13] using a Flatté formula for  $f_0(980)$ . As a test of the resonance hypothesis, these data have been refitted allowing complete freedom for the real and imaginary parts of the  $f_0(980)$  amplitude in 10 equal bins of  $s_{\pi\pi}$  from 0.84 to 1.08  $\text{GeV}^2$ . Fig. 2(b) compares results (crosses indicating the errors) with the fit of [13] shown by the smooth curve. The errors allow for a mass resolution of  $\pm 4$  MeV, which has quite a large effect near the  $KK$  threshold.

It is clear from Fig. 2(b) that the phase shift of  $f_0(980)$  increases by  $\sim 90^\circ$  from  $\sim 900$  MeV to the  $KK$  threshold at 991 MeV (the average mass for  $K^+K^-$  and  $K^0\bar{K}^0$ ). This supports the resonance interpretation.

As a further test, the fit has been repeated using Eqs. (8) and (9), which improve on the Flatté formula. Also, separate thresholds have been included for  $K^+K^-$  and  $K^0\bar{K}^0$ . There is a small improvement of 23 in log likelihood (statistically 5.5 standard deviations). There is only a small shift in the second sheet pole, which moves from  $998.4 \pm 4 - i(17.2 \pm 4)$  MeV to  $(1003.9 - i16.5)$  MeV with identical errors. [For the second sheet pole, the signs of  $\rho_2$  and  $j_2$  are reversed; for the third sheet pole, they are as in Eq. (14)]. Because the parametrisation of the cusp is now included, the distant third sheet pole moves from  $(851 - i418)$  MeV to  $(1171 - i592)$  MeV; this is because the cusp formula modifies the shape of the resonance away from the  $KK$  threshold.

It is of interest to use the  $f_0(980)$  as a model to examine the movement of the second-sheet pole as the parameters of the resonance are varied. This reveals the general features of the way the resonance forms. These general features are likely to be similar for other cases.

M (GeV)	$g_2^2$ (GeV <sup>2</sup> )	Pole (MeV)
0.956	0.895	778 - $i$ 42
	1.095	825 - $i$ 36
	1.295	858 - $i$ 31
	1.595	892 - $i$ 25
	0.695	710 - $i$ 48
	0.495	605 - $i$ 52
	0.295	438 - $i$ 44
	0.195	318 - $i$ 24

Table 1: Movement of the second sheet pole of  $f_0(980)$  with  $g_2^2$  using a pure cusp formula.

A fundamental point is whether the cusp alone can produce a pole at or very close to the  $KK$  threshold. The answer is no. For this test, the term  $-s$  of the Breit-Wigner denominator, Eq. (14), is removed, again including  $KK$  mass differences. A second sheet pole does appear, but well below the  $KK$  threshold. Table 1 shows the pole position for a variety of values of  $g_2^2$ . For small  $g_2^2$ , the pole moves rapidly away from the  $KK$  threshold. The reason the pole always lies below the  $KK$  threshold is that it is closely related to the term  $2|k_2|/\sqrt{s}$  of Eq. (11) which increases below the  $KK$  threshold with  $|k_2|$ .

The conclusion is that formation of the resonance requires an additional source of attraction, e.g. meson exchanges. Janssen et al. [16] were able to generate a resonance from  $K^*$  and  $\rho$  exchanges between  $\pi\pi$  and  $KK$ . Likewise, the  $\sigma$  and  $\kappa$  poles appear from meson exchanges in the calculations of Caprini et al. [17] and Büttiker et al. [18] using the Roy equations.

The attraction due to these long-range forces makes the real part of  $D(s)$  pass through 0 at some mass. It is of interest to see how effective the cusp is in attracting the second sheet pole when this crossing point varies. Table 2 shows the pole position as  $M$  of the Breit-Wigner formula is varied. From the first few entries, one sees that the pole moves a long way if  $M$  is far from the  $KK$  threshold. The cusp is effective in attracting the resonance over a mass range much larger than the  $\pi\pi$  width. From  $M = 0.9$  to 1.10 GeV, the pole stays quite close to the  $KK$  threshold. For  $M$  outside the range 0.5 to 1.1 GeV, it disappears. The pole is more easily pulled up to the  $KK$  threshold than down to it. Over the range of values in the Table, the distant third sheet pole moves only by small amounts.

The bottom entries in the Table show how the second sheet pole varies with  $g_1^2$ . As it decreases, the width of the pole decreases more rapidly; as  $g_1^2 \rightarrow 0$ , it becomes a bound state 0.15 MeV below the  $K^+K^-$  threshold (the lower of the two  $KK$  thresholds). This bound state survives unchanged for zero  $g_1^2$  for any value of  $M$  over the range 0.5 to 1.1 GeV and beyond.

The general pattern which emerges is that a cusp superimposed on attraction due to either meson exchanges or quark confinement can lock the resonance close to the threshold for a wide range of parameters  $M$  and  $g_2^2$ . The cusp acts as a trigger for the resonance. This is particularly the case when  $g_1^2$  is small. The locking mechanism is obviously inhibited if there is repulsion in meson exchanges.

Törnqvist [3] gives a formula for the  $KK$  component in the wave function of any resonance

M (MeV)	$g_1^2$ (GeV <sup>2</sup> )	Pole (MeV)
0.50	0.185	806 - <i>i</i> 76
0.60		852 - <i>i</i> 68
0.70		899 - <i>i</i> 59
0.80		946 - <i>i</i> 48
0.85		968 - <i>i</i> 41
0.90		987 - <i>i</i> 31
0.94		1000 - <i>i</i> 21
0.956		1004 - <i>i</i> 17
0.97		1007 - <i>i</i> 12
0.99		1011 - <i>i</i> 4
1.01		1012 - <i>i</i> 4
1.03		1012 - <i>i</i> 15
1.05		1009 - <i>i</i> 28
1.10		979 - <i>i</i> 69
0.956	0.285	1023 - <i>i</i> 32
	0.1	993 - <i>i</i> 7
	0.05	989 - <i>i</i> 3
	0.02	988 - <i>i</i> 0.8
	0	987.2

Table 2: Movement of the second sheet pole of  $f_0(980)$  from Eqs. (8) and (9) as its parameters are varied. In all cases,  $g_2^2 = 0.875 \text{ GeV}^2$ .

close to a threshold. For the present case, it may be written:

$$\psi = \frac{|q\bar{q}q\bar{q}\rangle + \sum_i [(d/ds)\text{Re}\Pi_i(s)]^{1/2} |KK\rangle}{1 + \sum_i (d/ds)\text{Re}\Pi_i(s)}; \quad (19)$$

this was evaluated in Ref. [19] and gives  $\sim 60\%$   $KK$  component for  $f_0(980)$ . That reference also shows that decay branching ratios favour an abnormally large  $KK$  component in  $f_0(980)$ .

Model calculations of a similar nature have been made by van Beveren and Rupp [20]. They adopt a transition potential coupling confined states in a harmonic oscillator potential to outgoing waves, with a matching at the transition radius  $\sim 0.65 \text{ fm}$ . The  $\sigma$ ,  $\kappa$ ,  $a_0(980)$  and  $f_0(980)$  emerge from the continuum as their coupling constant to confined states is increased. The great merit of their model is that it is straightforward to follow the movement of poles as this coupling constant varies. They give graphic illustrations of the movement of the  $\kappa$  and  $a_0(980)$  poles with coupling constants. The movement of the  $\sigma$ ,  $\kappa$ ,  $a_0(980)$  and  $f_0(980)$  poles as a function of coupling constant is also tabulated in Ref. [21]. The model reproduces fairly well the amplitudes for all these states with a universal coupling constant. The  $a_0$  does not appear at the  $\eta\pi$  threshold because of the nearby Adler zero. The  $\sigma$ ,  $\kappa$  and  $a_0$  all become bound states if the coupling constant is increased by a factor 2.5.

Jaffe proposes that mesons can be divided into ‘ordinary mesons’ which decouple from scattering channels as the number of colours  $N_c \rightarrow \infty$  and ‘extrordinary mesons’ which disappear

in this limit [22]. He draws attention to the work of Pelaez on the  $N_c$  dependence of the chiral Lagrangian and its predictions for low mass  $\pi\pi$  scattering [23].

A final comment is that the phase shift for  $\sigma$  goes through  $90^\circ$  very close to the  $KK$  threshold. This may not be accidental. The  $\sigma$  has significant coupling to  $KK$  and it is possible that the cusp mechanism is sufficient to tie the  $90^\circ$  phase to the threshold as well as that of  $f_0(980)$ .

## 4 $X(3872)$

Fig. 3 shows  $j_2$  and  $\rho_2$  for the  $\bar{D}D^*$  threshold. The result is similar to Fig. 1. Attempts to fit the data with a bare cusp (i.e. with  $M^2 - s$  of the denominator replaced with just  $M^2$ ) can reproduce the very narrow width observed in decays to  $\rho J/\Psi$  only with very fine tuning of parameters. There is then a second sheet pole almost at the  $D\bar{D}^*$  threshold. However this narrow width is incompatible with data on decays to  $\bar{D}D^*$  shown below in Fig. 4. The conclusion is that a resonance or virtual state is required

The cusp can however capture a nearby  $c\bar{c} \ ^3P_1$  state. The alternative possibility is a molecule generated by  $\pi$  exchange.

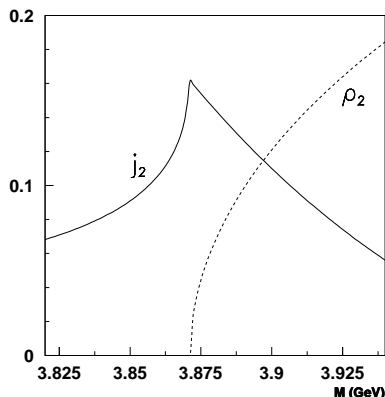


Figure 3:  $j_{\bar{D}D^*}(s)$ ,  $\rho_{\bar{D}D^*}(s)$  for  $X(3872)$ ; the vertical scale is arbitrary.

The data with the best mass resolution are from Belle and Babar on decays to  $\rho J/\Psi$  [24] [25] and  $\bar{D}D^*$  [26] [27]. These have been fitted by Braaten and collaborators [29] and by Hanhart et al. [30]. They favour respectively a weakly bound state and a virtual state. Both omit the dispersive effect discussed here, but assume an attractive interaction which generates a nearby second sheet pole.

It is necessary to fit the narrow width observed in  $\rho J/\Psi$  simultaneously with the  $\sim 3.5$  MeV mass difference between the peaks observed there and in  $\bar{D}D^*$ . The Belle data are shown in Fig. 4 with a variety of fits. For  $\rho J/\Psi$  the improved data set shown by Olsen is used [31].

The mass distribution in  $\rho J/\Psi$  (taken as channel 1) and  $\bar{D}D^*$  (channel 2) are:

$$\frac{dN_1}{ds} = \Lambda \frac{G_1^2 \rho_1(s)}{|D(s)|^2} \quad (20)$$

$$\frac{dN_2}{ds} = \Lambda \frac{G_2^2 \rho_2(s)}{|D(s)|^2} \quad (21)$$

$$D(s) = M^2 - s - iM(\Gamma_1 + g_2^2[\rho_1(s) + j_2/i]) \quad (22)$$

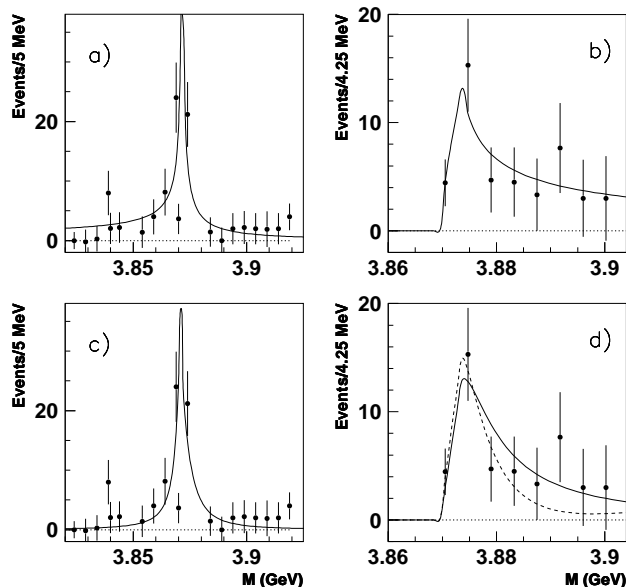


Figure 4: Fits to Belle data for (a) and (c)  $X(3872) \rightarrow \rho J/\Psi$ , (b) and (d)  $\bar{D}D^*$ ; the upper panels are fitted with a virtual state and the lower two with a resonance.

for a resonance; for a virtual state,  $-s$  in  $D(s)$  is replaced by  $-\gamma k_2^2$ . The parameter  $\Lambda$  is an overall normalisation constant. A constant  $\Gamma_1$  describes the width to channels other than  $\bar{D}D^*$ .

The peak in  $\bar{D}D^*$  is naturally higher in mass than in  $\rho J/\Psi$  because of the factor  $\rho_2$  in the numerator of Eq. (21). However the width of the  $J/\Psi$  peak cannot be too small if the difference in peak positions is to be accommodated. The branching ratio  $BR[\rho J/\Psi]/BR[\bar{D}D^*] = 0.08 \pm 0.04$  including allowance for  $D^* \rightarrow D\gamma$  as well as  $D\pi$ . The branching ratio  $BR[\omega J/\Psi]/BR[\rho J/\Psi] = 1.0 \pm 0.4 \pm 0.3$  [32]. A fit with these decay modes gives only a 1.5 MeV mass difference between  $\rho J/\Psi$  and  $\bar{D}D^*$ , but is sensitive to the assumed mass resolution; here a moving average is calculated over the 4.25 MeV bins quoted by Belle for  $\bar{D}D^*$  data.

There may well be other unobserved decays, e.g. to  $[\chi_1\sigma]_{L=0}$  and/or  $[\eta_C\sigma]_{L=1}$ , where  $L$  is the orbital angular momentum in the decay; they would be hard to detect experimentally. Contributions from these channels seem likely since decays to  $\rho J/\Psi$  are isopin violating and the phase space for  $\omega J/\Psi$  is very limited. The splitting between  $\rho J/\Psi$  and  $\bar{D}D^*$  peaks is easily increased to 3 MeV by allowing extra decay channels with a rate a factor 4-8 larger than  $\rho J/\Psi + \omega J/\Psi$ .

Figs. 5(a) and (b) show fits with a virtual state; Figs. 5(c) and (d) use a resonance. There is little to choose between them. Presently the only way of making a definite distinction would be to determine the phase directly from interferences with other components in Dalitz plots; the virtual state has a falling phase above the peak. A minor detail is that Fig. 4(d) show a second fit as a dashed curve, assuming there is some background in  $\bar{D}D^*$  at high masses. In view of the uncertainties, a full list of fitting parameters is not useful. For the full curve of Fig. 4(d),  $M = 3871.8$  MeV,  $\Gamma = 8$  MeV and equal branching ratios are used to  $\bar{D}D^*$  and the sum of other channels. The full-width at half-maximum is however only 4.3 MeV because of the cusp contribution to the resonance.

Belle report a peak in  $\bar{D}D^*$  at  $3942_{-6}^{+7} \pm 6$  MeV with  $\Gamma = 37_{-18}^{+26} \pm 8$  MeV [28]. A spin-

parity analysis is important. It could be the  ${}^3P_1$  radial excitation, in which case  $X(3872)$  is to be interpreted as a molecular state generated by the cusp mechanism and attractive meson exchange. Alternatives are  $J^P = 0^-, 1^-$  or  $2^-$ , though these would be suppressed near the  $\bar{D}D^*$  threshold by an  $L = 1$  centrifugal barrier for decay.

## 5 $Z(4430)$

The  $Z^+(4430)$  observed recently by Belle is important as a clear candidate for an exotic meson. It appears at the  $\bar{D}^*(2010)D_1(2420)$  threshold within errors. It has a modest width  $\sim 44$  MeV comparable with the width of  $D_1$  itself ( $25 \pm 5$ ) MeV.

Unlike  $X(3872)$  it has many likely de-excitation processes

- $0^- \rightarrow [D\bar{D}_0(2308)]_{L=0}, [D\bar{D}^*]_{L=1}$  and  $[D^*\bar{D}^*]_{L=1},$
- $1^- \rightarrow [D^*\bar{D}_0(2308)]_{L=0}, [D\bar{D}]_{L=1}, [D\bar{D}^*]_{L=1}$  and  $[D^*\bar{D}^*]_{L=1},$
- $2^- \rightarrow [D\bar{D}^*]_{L=1}$  and  $[D^*\bar{D}^*]_{L=1}.$

The essential point is that these de-excitation processes unavoidably lead to a strong threshold cusp unless meson exchanges are repulsive for all  $J^P$ .

It is necessary to fold the width of the  $D_1(2420)$  into the calculation of the cusp. Consider as an example decays of  $D^*(2010)D_1(2420)$  to  $D^*(2010)D(1865)$  with  $L = 1$ . For fixed total  $s$  of the initial state and fixed mass  $s_1$  of  $D_1$ , the intensity is proportional to  $(2k_1/\sqrt{s})B_1(k_1R)F^2(k_1R)$  (ignoring the very small widths of  $D$  and  $D^*$ ); here  $k_1$  is the centre of mass momentum in the final state and  $B_1 = k_1^2R^2/(1 + k_1^2R^2)$  is the centrifugal barrier factor for  $L = 1$  decay. Since  $k_1$  is large ( $\sim 1070$  MeV/c),  $B_1 \simeq 1$ . Including the phase space for the initial state and integrating over the line-shape of  $D_1(2420)$ , the phase space factor for the whole process is

$$\rho(s) = \int_{(M_D+M_{D^*})^2}^{(\sqrt{s}-\sqrt{s_1})^2} ds_1 \frac{F^2(k_2R)}{|D(s_1)|^2} \frac{4k_2k_1}{\sqrt{ss_1}} F^2(k_1R), \quad (23)$$

where  $k_2$  is the momentum in the  $D^*\bar{D}_1$  channel. This integral is easily done numerically. The important dependence is on  $k_2$ ,  $F^2(k_2R)$  and  $D(s_1)$ .

Fig. 5(a) show the result for  $\rho(s)$  and its dispersion integral  $g^2j(s)$  with a subtraction at 3.95 GeV, well below the  $D^*\bar{D}_1$  threshold. The full curves of Fig. 5 show  $\rho(s)$  (normalised to 1 at its peak) and its dispersion integral  $g^2j(s)$  (normalised accordingly). The dashed curve shows the result of a large change in  $F^2$  to  $\exp(-6k_2^2)$ .

The Belle data show a  $Z(4430)$  peak accurately coincident with the  $\bar{D}D^*$  threshold. The data can easily be reproduced as a resonance, and the fit is shown in Fig. 5(b). Close [33] argues in favour of binding by  $\pi$  exchange, though Liu et al. reach the opposite conclusion [34]. Li, Lü and Wang raise the interesting possibility of a nonet of strange relatives at the  $D_s^*(2112)\bar{D}_1(2420)$  and  $D^*\bar{D}_{s1}$  thresholds near 4540 MeV and the  $D^*D_{s1}$  threshold at 4647 MeV.

The width of  $D_1(2420)$  reduces the sharpness of the cusp, though this could be more than compensated by the large number of decay channels into which  $D^*\bar{D}_1$  may de-excite. A cusp plus meson exchange could generate an exotic resonance, but the net attraction must overcome zero-point energy. We proceed to test whether an alternative fit is possible using a bare cusp.

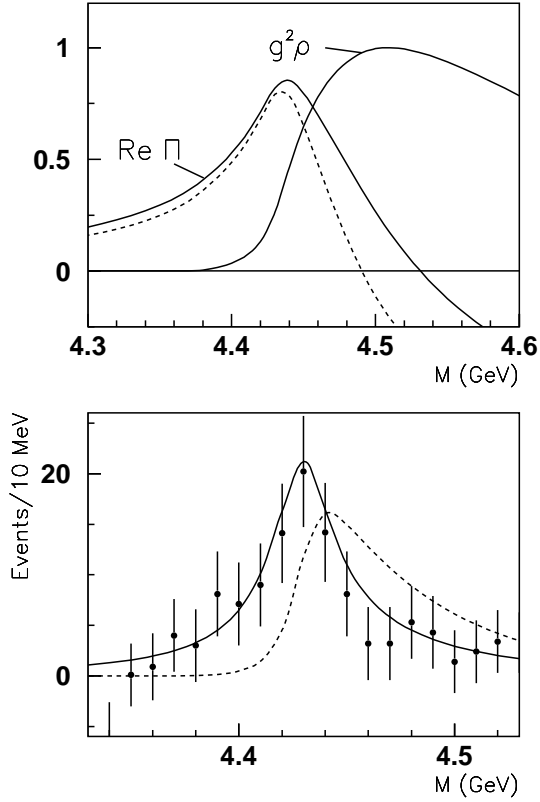


Figure 5: (a)  $g^2(D^*\bar{D}_1)$  and  $\text{Re}\Pi(D^*\bar{D}_1)$  calculated from de-excitation of  $D^*\bar{D}_1$  to  $[D^*\bar{D}]_{L=1}$ . The dotted curve shows the effect of doubling the exponent of the form factor. (b) Fit to Belle data with a resonance; the dashed curve shows the predicted peak in  $D^*\bar{D}_1$ , but scaled upwards for visibility

## 5.1 A subtlety in the equations

At this point, a digression is needed to discuss a missing element in Törnqvist's equations. For a 2-channel system (which is sufficient to reveal the essential point), the usual expression relating the  $T$ -matrix and  $K$ -matrix elements is:

$$T\rho = \frac{1}{B} \begin{pmatrix} k_{11} & k_{12} \\ k_{21} & k_{22} \end{pmatrix} \begin{pmatrix} (1 - ik_{22}) & -ik_{12} \\ -ik_{21} & (1 - ik_{11}) \end{pmatrix} \quad (24)$$

$$B = 1 - ik_{11} - ik_{22} + (k_{12}k_{21} - k_{11}k_{22}), \quad (25)$$

where  $k_{ij} = \sqrt{k_i k_j} a_{ij}$ . Using time-reversal invariance,  $k_{12} = k_{21}$ . Then

$$T_{22}\rho_2 = \frac{a_{22}\rho_2 - i\rho_1\rho_2(a_{12}^2 - a_{11}a_{22})}{1 - ia_{11}\rho_1 - ia_{22}\rho_2 + \rho_1\rho_2(a_{12}^2 - a_{11}a_{22})} \quad (26)$$

$$T_{12}\sqrt{\rho_1\rho_2} = \frac{a_{12}\sqrt{\rho_1\rho_2}}{1 - ia_{11}\rho_1 - ia_{22}\rho_2 + \rho_1\rho_2(a_{12}^2 - a_{11}a_{22})}, \quad (27)$$

$T_{11}$  is like  $T_{22}$  with indices interchanged. In order to arrive at a form  $T = N/D$  where  $N$  is real, it is necessary to multiply top and bottom of  $T_{22}$  and  $T_{11}$  by the complex conjugate of the

numerator. Note that the resulting denominator  $D$  is then different from that of  $T_{12}$ . So the result does not describe a resonance, for which  $D$  should be common to all channels. For all denominators to be the same, the requirement is that  $a_{12}^2 - a_{11}a_{22} = 0$ . This is satisfied at a pole. This term was omitted by Törnqvist and from the equations of Section 2 because there are indeed second sheet poles very close to the experimental peaks. In general however, this term is not zero. If it is completely dominant,  $T_{11}\rho_1$  and  $T_{22}\rho_2 \rightarrow i$ . In particular, this arises if  $T_{12}$  is large. That is to be expected for de-excitation of  $D^*\bar{D}_1$  to many  $D\bar{D}$  channels with lower thresholds.

Fig. 6(b) shows the fit to Belle data with a bare cusp and Fig. 6(a) shows the Argand diagram for  $T_{12}$ . Below threshold, the cusp effect creates attraction, pulling all amplitudes around the periphery of the unitary circle towards the threshold. At the threshold, the amplitude curls towards the centre of the Argand diagram. As the inelasticity grows, amplitudes for individual decay channels move back to the origin, though their total goes to  $i$ . For this fit, there is no second or third-sheet pole anywhere in the vicinity of the cusp.

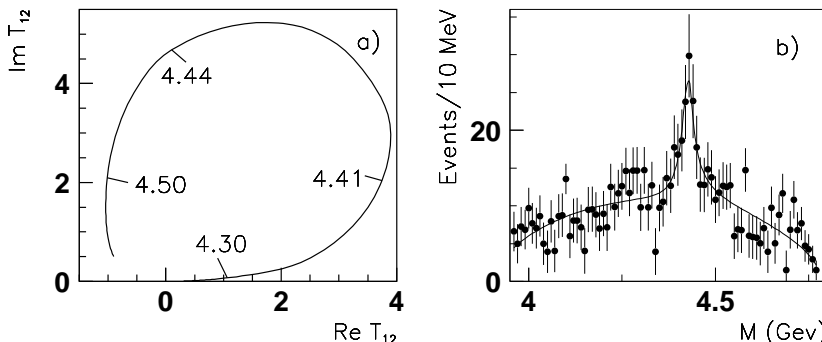


Figure 6: Fit with a bare cusp: (a) Argand diagram, (b) fit to Belle data

Some further detail is needed on exactly how data are fitted. The tails of a cusp depart somewhat from a resonance form. To allow for this, it is necessary to make small adjustments to the background fitted by Belle. This background is taken to be linear in  $s$  (slightly higher at low  $s$  than high  $s$ ), multiplied by the phase space factors  $Q_1$  for  $Z \rightarrow \psi'\pi$  and  $Q_2$  for  $B \rightarrow KZ$ . The calculation of  $a_{ij}$  is done for  $Z \rightarrow [\bar{D}D^*]_{L=1}$  as a representative example. The dispersion integral is strictly over  $\rho_1\rho_2$ , but the dependence on  $\rho_1$  is in practice small. It is assumed that  $a_{12} \gg a_{22}$  though the coupling constant to  $\bar{D}D^*$  is fitted explicitly and so is  $a_{11}$ , which is taken as a constant since it is insensitive to form factors. The denominator of  $T_{12}$  for the  $\Psi'\pi$  channel is the same as for all other channels.

How can experiment resolve a cusp from a resonance? The difference in line-shape is small and easily confused with experimental backgrounds. The essential feature of a resonance is that the phase shift increases by  $90^\circ$  up to the centre of the cusp. The detailed  $s$ -dependence on Fig. 6(a) is different from a resonance, but the difference is delicate. This can in principle be measured from interference with other components in the Dalitz plot, but would require a large increase in statistics.

The  $Z(4430)$  may be a resonance. The Argand diagram of Fig. 6(a) resembles a resonance. If meson exchanges are attractive, it is quite possible that they will combine with the cusp mechanism to generate a resonance. Mixing with a genuine diquark-antidiquark system is less

likely, since the long-range tail of the wave function must be purely molecular.

## 5.2 Other points

Rosner and also Meng and Chao remark on the experimental fact that no signal is seen for  $Z(4430) \rightarrow J/\Psi\pi$  despite larger phase space. This may be due to a cancellation in the matrix element for  $D^*\bar{D}_1 \rightarrow J/\Psi\pi$ . The momenta for production of  $J/\Psi$  and  $\Psi'$  are large: 1130 and 670 MeV/c respectively. The  $J/\Psi$  and  $\Psi'$  wave functions are multiplied by a factor  $\exp(ikr)$  which has nodes at 0.27 or 0.43 fm in the two cases.

In more detail, the matrix element for  $Z \rightarrow \Psi'\pi$  in the rest frame of the  $\Psi'$  is

$$M = \int_0^\infty r^2 dr \Psi'(r) [j_1(kr) \cos \delta + n_1(kr) \sin \delta], \quad (28)$$

using for the initial state the long-range part of its wave function, expressed in terms of spherical Bessel and Neumann functions. This is only a first approximation and the short range part of the wave function is unknown. The appearance of  $n_1 \sin \delta$  signifies the fact that the radial wave function is sucked in by the attractive interaction due to the cusp, causing the phase shift  $\delta$ . For a strong cusp due to many open channels,  $n_1 \sin \delta$  should dominate. For the kinematics of  $J/\Psi$  production,  $n_1$  has a node at 0.38 fm, leading to a distinct cancellation within the matrix element. For  $\Psi'$  production,  $n_1$  has a node at 0.64 fm. This gives a reasonable overlap with the expected wave function for  $\Psi'$ , though by no means perfect. This discussion is only semi-quantitative because actual radial wave functions are unknown, but provides some explanation why the decay to  $J/\Psi\pi$  may be weak.

The next task for experiment is a spin analysis of  $Z(4430)$ , so expressions will be given for partial waves. It is highly desirable to use the amplitude for the full process  $B \rightarrow K\Psi'\pi$ ; both production and decay in principle determine  $J^P$ , but angular correlations between them provide further delicate information which constrains the analysis strongly. My experience is that 100 fully analysed events achieve the same significance level (in terms of  $\chi^2$  of the fit to data) as 400–800 events where only information from decays is used.

Formulae simplify greatly in the rest frame of the  $Z(4430)$ . There, the angular momentum of the kaon in the production reaction is expressed by its 3-momentum  $\vec{K}$ . Likewise, the angular momentum of the pion in the decay  $Z \rightarrow \psi'\pi$  is given by its 3-momentum  $\Pi$ . However, a small correction is required for the Lorentz transformation of  $\Psi'$  spin between its rest frame and that of  $Z(4430)$ . Suppose the  $xz$  plane is defined by the recoil pion and leptons from the decay of  $\Psi'$ . Let  $R$  be the angle between the (unmeasured) polarisation vector and this plane. In this plane, let  $\theta$  be the angle between the lepton axis and the pion in the rest frame of  $\Psi'$ . The polarisation vector  $e$  of the  $\Psi'$  is orthogonal to the lepton axis in the  $\Psi'$  rest frame and may be written as a 4-vector  $e = [\cos R, \sin R, 0, 0]$ . The intensity is obtained using  $\langle \cos^2 R \rangle = \langle \sin^2 R \rangle = 1/2$ . A simple trick avoids this integration. The  $e_x$  and  $e_y$  components may be replaced by  $1/\sqrt{2}$  and  $i/\sqrt{2}$ . Intensities are then obtained by taking the modulus squared of matrix elements. Appendix 1 of [35] shows that the Lorentz boost between the rest frames of  $\Psi'$  and  $Z(4430)$  gives a polarisation vector  $e' = (1/\sqrt{2})[1 + (\gamma - 1) \sin^2 \theta, i, \sin \theta \cos \theta (1 - \gamma)i, \beta \gamma \sin \theta \cos \theta]$ , where  $\beta$  and  $\gamma$  are the usual parameters of the Lorentz transformation. In the  $Z$  rest frame, the fourth component of  $e'$  drops out of all matrix elements. Numerically,  $(\gamma - 1) = 0.064$ , so the effect of the Lorentz boost is small.

After this preliminary, expressions for matrix elements  $M$  in the  $Z$  rest-frame are simple. For  $J^P = 0^-$ ,  $M = e' \cdot \Pi$  and  $K$  does not contribute. The choice of  $xz$  plane gives  $\Pi_y = 0$ , so the angular distribution is  $d\sigma/d\Omega \propto (e'_x \Pi_x)^2 + (e'_z \Pi_z)^2 \simeq \Pi_x^2$ . If the small term in  $(\gamma - 1)^2$  is dropped, this is proportional to  $\sin^2 \theta$ , as Rosner remarks.

For  $J^P = 1^-$ ,  $M \propto K \cdot e' \wedge \Pi = -e' \cdot K \wedge \Pi$ , so the kaon and pion are preferentially orthogonal in the rest frame of  $Z$ . For  $J^P = 2^-$ ,  $M \propto \tau_{\alpha\beta} T^{\beta\alpha}$ , where  $\tau_{\alpha\beta} = K_\alpha K_\beta - (1/3)(K_x^2 + K_y^2 + K_z^2)$ , representing  $L = 2$  for the kaon;  $T_{\alpha\beta} = e'_\alpha \Pi_\beta + e'_\beta \Pi_\alpha - (2/3)(e'_x \Pi_x + e'_z \Pi_z)$ , remembering that  $\Pi_y = 0$ . If only one spin is present,  $\sim 100$  events may well be sufficient to identify the spin. More than one spin would suggest a non-resonant cusp.

## 6 Other cases

The association of some peaks with thresholds may be numerical accidents. Hence examples discussed here are not comprehensive, but concentrate on cases where the agreement is remarkably close or is otherwise of special interest.

A narrow peak is observed in  $D^0 p$  by Babar [36] and Belle [37] with a mass of  $2939.8 \pm 1.3 \pm 1.0$  MeV and  $\Gamma = 17.5 \pm 5.2 \pm 5.9$  MeV and also in  $\Sigma_C(2455)\pi$ . Its mass is just below the  $D^0 p$  threshold at  $2944.9 \pm 0.4$  MeV. For an S-wave threshold,  $J^P = (1/2)^-$  or  $3/2^-$ . It could be a molecular state [38]; alternatively a nearby regular  $\Lambda_C$  state may be captured by the  $D^0 p$  threshold.

The  $\Lambda_C^+(2595)$  has a mass of  $2595.4 \pm 0.6$  MeV [39], very close to that of  $\Sigma_C^{++}\pi^-$ , namely 2593.6 MeV. It is too narrow to be a pure cusp, but may be a resonance attracted to the threshold where decays to  $\Lambda_C \pi$  are possible.

The  $\Psi(4039)$  lies close to the  $D^* \bar{D}^*$  threshold at 4014 MeV. However, it has a width of  $80 \pm 10$  MeV, making its association with a cusp effect questionable. Dunynskiy and Voloshin discuss in detail the complicated dependence on mass of  $D^* \bar{D}^*$ ,  $D^0 \bar{D}^0$  and  $D_s \bar{D}_s$  channels [40].

The  $D_s(2315)$  is very narrow and  $\sim 50$  MeV below the  $D \bar{K}$  threshold. It is therefore unlikely to be a molecular state, though it could be an example of a diquark-antidiquark configuration. In the absence of other clear examples of strongly bound 4-quark systems, the likely explanation is a  $c\bar{s}$  state.

Amongst the light mesons, the  $f_2(1565)$  has a phase variation which is well determined by Crystal Barrel data on  $\bar{p}p \rightarrow 3\pi^0$  at rest. Those data have been fitted simultaneously with data on  $\bar{p}p \rightarrow \omega\omega\pi^0$  at rest [41] and definitely require a resonance accurately at the  $\omega\omega$  threshold. The  $f_2(1640)$  reported by the Particle Data Group is the decay to  $\omega\omega$ , which is moved upwards from 1565 MeV by  $\omega\omega$  phase space. There is no other candidate for the radial excitation of  $f_2(1565)$ , so it appears that this state has been captured by the  $\omega\omega$  threshold. Note, however, that the well known  $f_0(1500)$  is not attracted to that threshold; its decays into  $\omega\omega$  are weak.

The  $\rho(1900)$  of the Particle Data Tables has a rather narrow width. This is suggestive of a cusp due to the strong  $\bar{p}p$  threshold.

The  $\pi_1(1400)$  could be a bare cusp. It has been assumed by most groups to be a resonance. However, it is close to the  $f_1(1285)\pi$  and  $b_1(1235)\pi$  thresholds, which would appear in S-wave decays. Dzierba et al. question whether it is a threshold effect or a resonance [42]. The  $\pi_1(1600)$  appears at higher mass with the same quantum numbers and is observed dominantly in  $b_1(1235)\pi$  and less strongly in  $f_1(1285)\pi$ . So the  $\pi_1(1400)$  could be a molecular configuration coupled to

these thresholds or could be simply a cusp effect. A full analysis is needed of the two alternatives using analytic forms like those presented here. The data on  $\bar{p}p \rightarrow \pi^0\pi^0\eta$  show only a very weak signal in the  $\eta\pi$  P-wave, insufficient to tell the difference between the two alternatives [43].

Valcarce, Vijande and Barnea have made an interesting study of mixing between diquark and tetraquark configurations [44], though they do not specifically take the cusp effect into account.

## 6.1 $X(1812)$

An intriguing case is the sharp  $\omega\phi$  signal reported by the BES collaboration [45], peaking at 1812 MeV, just above the  $\phi\omega$  threshold at 1801 MeV. If it were purely a threshold effect, it should peak considerably higher. It is therefore very likely associated with the  $f_0(1790)$ , a resonance clearly separated from  $f_0(1710)$  in BES data on  $J/\Psi \rightarrow \omega KK$  [46] and  $\phi\pi\pi$  [11]. Data on the  $\omega KK$  channel display a strong  $f_0(1710)$  peak, but nothing is visible in  $\omega\pi\pi$ , despite large statistics. Conversely, the  $f_0(1790)$  appears clearly in  $\phi\pi\pi$ , but any  $\phi KK$  signal is weak. There is a factor 22 difference in decay branching ratios to  $\pi\pi$  and  $KK$ , hence requiring separate  $f_0(1710)$  and  $f_0(1790)$ . The  $f_0(1790)$  is also observed in  $J/\Psi \rightarrow \gamma 4\pi$  [47] [48]. It is accommodated naturally as the radial excitation of  $f_0(1370)$ .

The  $\phi\omega$  decay can arise naturally from a glueball component in  $f_0(1790)$  [49] [50]. A glueball is a flavour singlet. It has flavour content

$$F = (u\bar{u} + d\bar{d} + s\bar{s})(u\bar{u} + d\bar{d} + s\bar{s}). \quad (29)$$

If the decay is to vector mesons, the component  $(u\bar{u} + d\bar{d})(u\bar{u} + d\bar{d})$  makes three charge combinations of  $\rho\rho$  and one of  $\omega\omega$ . The component  $2(u\bar{u} + d\bar{d})s\bar{s}$  can make  $4\omega\phi$  or  $2(K^{*0}\bar{K}^{*0} + K^{*-}K^{*-})$  or some linear combination.

There are BES I data on  $J/\Psi \rightarrow \gamma(K^+\pi^-K^-\pi^+)$  showing that the channel  $\gamma(K^*\bar{K}^*)$  does not contain any significant  $0^+$  signal [51]. The paper says: ‘Contributions from  $0^{++}$  and  $4^{++}$  are small or absent’. A signal with the same magnitude as that of  $J/\Psi \rightarrow \gamma(\omega\phi)$  in [45] would be rather conspicuous near 1800 MeV, because of the small phase space at that mass for  $K^*\bar{K}^*$ . Its absence there may be qualitatively attributed to the fact that  $(u\bar{u} + d\bar{d})s\bar{s}$  has larger phase space in  $KK$  decays than  $K^*\bar{K}^*$ .

## 7 Concluding Remarks

A sharp threshold generates a cusp in the real part of scattering amplitudes at the opening of a new threshold. This is a dispersive effect, arising from analyticity. If there is an attractive  $t$ - or  $u$ -channel exchange, it can add coherently to the cusp effect and generate a resonance. The  $f_0(980)$  appears to behave in this way. The cusp can also add coherently to the confinement ‘potential’ and attract a regular quark resonance to the threshold. This explains why states like  $f_2(1565)$ ,  $K_0(1430)$  and  $\Lambda_C(2940)$  appear at thresholds.

At the threshold, zero point energy is minimised by the long-range tail of the wave function. Mixing between quark configurations and meson-meson states minimises the energy of the linear combination in a way analogous to the formation of a covalent bond in chemistry.

Diquark-antidiquark resonances may exist. However, if they lie close to a threshold, zero-point energy will necessarily mix a large molecular component into the wave function. The  $f_0(980)$ ,

for example, has a component of  $\sim 60\%$  KK. Section 2 used known parameters of  $f_0(980)$  to examine how the second-sheet pole position is affected by perturbations to its parameters. The conclusion is that the cusp mechanism can attract a resonance over a surprisingly large mass interval of order  $\pm 100$  MeV. If the open channel ( $\pi\pi$ ) is switched off, the resonance becomes a bound-state pole just below threshold.

The  $X(3872)$  is too narrow to be fitted as a pure cusp. Although parameters of the cusp can be fine-tuned to fit the line-shape observed in decays to  $\rho J/\Psi$ , they then fail to reproduce the peak observed 3.5 MeV higher in  $\bar{D}D^*$  decays. Both peaks may be fitted with a resonance or virtual state. A definitive distinction between these possibilities requires phase information from interferences in Dalitz plots: for a virtual state, the phase falls above the threshold. The natural explanation of  $X(3872)$  is that the  $\bar{s}s$   $^3P_1$  radial excitation has been attracted to the  $\bar{D}D^*$  threshold. The weak decays of  $c\bar{c}$  to non  $\bar{D}D$  channels like  $\rho J/\Psi$ ,  $\omega J/\Psi$ ,  $[\chi\sigma]_{L=0}$  and  $[\eta_C\sigma]_{L=1}$  lead to a very narrow resonance.

The  $Z(4430)$  can be fitted as a resonance. It is quite possible that meson exchanges generate sufficient attraction to turn the cusp into a resonances. However, it cannot presently be excluded that a non-resonant cusp fits the data using equations (26) and (27). The availability of many de-excitation channels such as  $[\bar{D}D^*]_{L=1}$  necessarily produces a strong cusp. Partial wave formulae to assist separation of spin-parity assignments  $0^-$ ,  $1^+$  and  $2^-$  are given in Section 4. The presence of more than one  $J^P$  would suggest a bare cusp.

Equations (8), (9) and (14) for a sharp threshold improve on the Flatté formula and are just as easy to use. The experimental data for  $f_0(980)$  conform with the line-shape predicted by these equations. However, as Törnqvist remarks, increasing the precision of the formula and its parameters may be an academic exercise. A case which does require study with full inclusion of the dispersive effect is  $\pi_1(1405)$ , which could be a resonance or could be just a threshold cusp.

## 8 Acknowledgements

I wish to thank Prof. G. Rupp and Prof. E. van Beveren for extensive discussions. Use of their model led to important insight into the way poles move near a threshold. It is recommended as a test-bed for quantitative studies. I also wish to thank Dr. Y. Kalashnikova for illuminating comments on the Flatté formula.

## References

- [1] Flatté S M 1976 *Phys. Lett.* **B 66** 224
- [2] Jaffe R 1977 *Phys. Rev.* **D 15** 267 and 281
- [3] Törnqvist N A 1995 *Z. Phys.* **C 68** 647
- [4] Törnqvist N A 2004 *Phys. Lett.* **B 599** 209
- [5] Close F E and Page P R 2003 *Phys. Lett.* **B 578** 119
- [6] Swanson E S 2004 *Phys. Lett.* **B 588** 189

- [7] Abe K *et al* (Belle Collaboration) 2007 *Preprint* arXiv: hep-ex/0708.1790
- [8] Rosner J L 2007 *Preprint* arXiv: hep-ph/0708.3496
- [9] Meng C and Chao K -T *Preprint* arXiv: hep-ph/0708.4222
- [10] Maiani L, Polosa A D and Riquer V 2007 *Preprint* arXiv: hep-ph/0708.3997
- [11] Ablikim M *et al* (BES Collaboration) 2005 *Phys. Lett.* **B 607** 243
- [12] Cabibbo N 2004 *Phys. Rev. Lett.* **93** 121801
- [13] Bugg D V 2007 *Euro. Phys. J* **C52** 55
- [14] Hyams B D *et al* 1973 *Nucl. Phys.* **B 54** 134
- [15] Abele A *et al* 1996 *Nucl. Phys.* **A 609** 562
- [16] Janssen G *et al* 1995 *Phys. Rev.* **D 52** 2690
- [17] Caprini I, Colangelo I and Leutwyler J 2006 *Phys. Rev. Lett.* **96** 032001
- [18] Büttiker P *et al* 2004 *Eur. Phys. J* **C 33** 409
- [19] Bugg D V 2006 *Eur. Phys. J* **C 47** 57
- [20] van Beveren E and Rupp G 2003 *AIP Conf Proc.* **660** 353
- [21] van Beveren E, Bugg D V, Kleefeld F and Rupp G 2006 *Phys. Lett.* **B 641** 265
- [22] Jaffe R 2007 *Preprint* arxiv: hep-ph/0701038
- [23] Pelaez J R 2004 *AIP Conf. Proc.* **688** 45; 2004 *Phys. Rev. Lett.* **92** 1020011; 2006 *AIP Conf. Proc.* **814** 670
- [24] Choi S K *et al* (Belle Collaboration) 2003 *Phys. Rev. Lett.* **91** 262001
- [25] Aubert B *et al* (Babar Collaboration) 2006 *Phys. Rev.* **D 73** 011101R
- [26] Gokhroo G *et al* (Belle Collaboration) 2006 *Phys. Rev. Lett.* **96** 162002
- [27] Aubert B *et al* (Babar Collaboration) 2007 *Preprint* arXiv: hep-ex/0708.1565
- [28] Pakhlov P *et al* (Belle Collaboration) 2007 *Preprint* arXiv: hep-ex/0708.3812
- [29] Braaten E and Lu M 2007 *Preprint* arXiv: hep-ph/0709.2697 and references cited there
- [30] Hanhart C *et al* 2007 *Phys. Rev.* **D 76** 034007
- [31] Olsen S L 2004 *Preprint* arXiv: hep-ex/0412068
- [32] Abe K *et al* (Belle Collaboration) 2005 *Preprint* arXiv: hep-ex/0505037

- [33] Close F E 2008 *Preprint* arXiv: hep-ex/0801.2646
- [34] Liu Z, Liu Y -R, Deng W -Z and Zhu S -L, *Preprint* arXiv: hep-ph/0711.0949
- [35] Bugg D V 2005 *Phys. Rev. D* **71** 016006
- [36] Aubert B *et al* (Babar Collaboration) 2007 *Phys. Rev. Lett.* **98** 012001
- [37] Mizuk R *et al* (Belle Collaboration) 2007 *Phys. Rev. Lett.* **98** 262001
- [38] He X G, Li X Q, Liu X and Zeng X Q, 2007 *Eur. Phys. J C* **51** 262001
- [39] Particle Data Group 2006 *J. Phys. G* **33** 1
- [40] Dubynskiy S and Voloshin M B 2006 *Mod. Phys. Lett. A* **21** 2779
- [41] Baker C A *et al* 1999 *Phys. Lett. B* **467** 147
- [42] Dzierba A R *et al* 2003 *Phys. Lett. D* **67** 094015
- [43] Bugg D V *et al* 1994 *Phys. Rev. D* **50** 4412
- [44] Valcarce A, Vijande J and Barnea N 2007 *Preprint* arXiv: hep-ph/0711.3114
- [45] Ablikim M 2006 *et al* (BES Collaboration) 2006 *Phys. Rev. Lett.* **96** 162002
- [46] Ablikim M *et al* (BES Collaboration) 2004 *Phys. Lett. B* **598** 149
- [47] Bugg D V *et al* 1995 *Phys. Lett. B* **353** 378
- [48] Bai J Z *et al* (BES Collaboration) 2000 *Phys. Lett. B* **472** 207
- [49] Bicudo P, Cotanch S R, Llanes-Estrada F J and Robertson T G (2007) *Eur Phys J C* **52** 363
- [50] Bugg D V (2006) *Preprint* arXiv: hep-ph/0603018
- [51] Bai J Z *et al* 2000 *Phys. Lett. B* **472** 200